INTERNATIONAL JOURNAL FOR NUMERICAL METHODS IN FLUIDS, VOL. 13, 287–307 (1991)

CHARACTERISTIC-BASED FLUX LIMITERS OF AN ESSENTIALLY THIRD-ORDER FLUX-SPLITTING METHOD FOR HYPERBOLIC CONSERVATION LAWS

HERNG LIN

Department of Power Mechanical Engineering, National Tsing Hua University, Hsinchu, Taiwan, Republic of China

AND

CHING-CHANG CHIENG

Department of Nuclear Engineering, National Tsing Hua University, Hsinchu, Taiwan, Republic of China

SUMMARY

A flux limiter based on characteristic variables is extended by a control volume flux formulation to approximate the convection term at the cell interface for an essentially third-order-accurate scheme. The basic algorithm uses implicit MUSCL-type flux splitting and the approximate factorization method. It is applied to three test problems: (i) a one-dimensional shock tube problem; (ii) a two-dimensional problem of an oblique shock step with Mach numbers 3 and 10 and a shock angle of 59°; (iii) a two-dimensional problem of transonic inviscid flow past an NACA0012 aerofoil with Mach number 0·8 at zero angle of attack. The computational results by the new flux limiter function are compared with the results of direct applications of the SMART algorithm, Leonard's SHARP algorithm, the third-order Van Leer flux-splitting method with a smooth limiter, Harten's second-order unwind-biased TVD scheme, Chakravarthy's third-order MUSCL-type TVD scheme and the exact solution. The comparison shows that the present method gives the most accurate and least oscillatory results with a rapid rate of convergence.

KEY WORDS Flux limiter Third-order-accurate scheme Flux-splitting method Control volume flux formulation Hyperbolic conservation laws

INTRODUCTION

For accurate high-order simulations of fluid flows with strong shocks, careful treatment of flow discontinuity is of great importance to avoid oscillatory solutions while achieving rapid convergence. Such investigations have been done with modern shock-capturing schemes, e.g. TVD, ENO and flux splitting. Total-variation-diminishing (TVD) schemes modify the numerical flux at the interface of a computational cell by use of various limiters to control the amount of antidiffusive flux.[1–6] The limiter is designed so that a conventional non-TVD scheme can be modified to satisfy the TVD conditions.[7] ENO schemes[8–10] use a piecewise polynomial as the interpolation technique, which helps to construct an essentially non-oscillatory solution from the cell average. For Steger–Warming splitting[11] the switching function, which is called a limiter, serves to limit the second-order term in the spatial differencing of the split flux, and the evaluation of the flux values at cell interfaces is crucial to the convergence rate and accuracy of the results. Anderson *et al.*[12] employed the MUSCL (monotone upstream central scheme for conservation

0271–2091/91/130287–21$10.50

Received July 1989
Revised August 1990

laws) approach instead of the standard flux difference of the Steger–Warming splitting method to evaluate the split flux at the interfaces and extended the model to a third-order upwind-biased model by a smooth limiter. The above-mentioned methods indicate that the estimation of the flux at interfaces is of common interest and important to the problems. In the meanwhile, the concept of control volume flux formulation in approximating the interface values is commonly used for convection–diffusion problems, e.g. the well–known TEACH code,[13] SMART[14] and the SHARP and QUICK algorithms of Leonard.[15,16] The present study effectively combines the concepts of flux limiter and control volume to form a new method.

The present study proposes an upwind–biased MUSCL-type scheme of Van Leer splitting with a new smooth limiter. The limiter is based on characteristic variables and is extended from the concept of control volume flux formulation of the SMART and SHARP algorithms, which deal only with the convection–diffusion equation of a single variable. This paper applies the concept to a system of variables and three problems are tested: (i) a one-dimensional shock tube problem; (ii) a two-dimensional problem of an oblique shock step with Mach numbers 3 and 10 and a shock angle of 59°; (iii) a two-dimensional problem of transonic inviscid flow past an NACA0012 aerofoil with Mach number 0·8 at zero angle of attack. The present method shows improvements in accuracy and convergence characteristics of the results when compared to other schemes such as modified SHARP, SMART and the Van Leer flux-splitting method.

MATHEMATICAL AND NUMERICAL MODELS

Governing equations

The governing equations are the time-dependent two-dimensional equations of ideal gas dynamics, i.e. the Euler equations. The inviscid conservation-law equations in Cartesian co-ordinates can be expressed in conservation form as follows:

$$\frac{\partial Q}{\partial t}+\frac{\partial F(Q)}{\partial x}+\frac{\partial G(Q)}{\partial y}=0, \tag{1}$$

where Q, $F(Q)$ and $G(Q)$ are the conserved variables and the convective fluxes. The conservation-law form of equation (1) can be maintained under the co-ordinate transformation

$$\xi=\xi(x,y), \qquad \eta=\eta(x,y) \tag{2}$$

and is expressed as

$$\frac{\partial \hat{Q}}{\partial t}+\frac{\partial \hat{F}}{\partial \xi}+\frac{\partial \hat{G}}{\partial \eta}=0, \tag{3}$$

where

$$\hat{Q}=\frac{Q}{J}=\frac{1}{J}\begin{bmatrix}\rho\\ \rho u\\ \rho v\\ E_t\end{bmatrix}, \qquad \hat{F}=\frac{1}{J}\begin{bmatrix}\rho U\\ \rho Uu+\xi_x p\\ \rho Uv+\xi_y p\\ (E_t+p)U\end{bmatrix}, \qquad \hat{G}=\frac{1}{J}\begin{bmatrix}\rho V\\ \rho Vu+\eta_x p\\ \rho Vv+\eta_y p\\ (E_t+p)V\end{bmatrix}. \tag{4}$$

The equations are non-dimensionalized in terms of the reference density ρ_∞ and speed of sound a_∞. The velocity components are u and v in the x- and y-directions respectively. The pressure p is related to the conserved variable Q through the equation of state given by

$$p=(\gamma-1)[E_t-\rho(u^2+v^2)/2], \tag{5}$$

where γ is the ratio of specific heats, taken as $\gamma = 1{\cdot}4$. The Jacobian of the transformation is denoted by J and can be expressed as $J = \xi_x \eta_y - \xi_y \eta_x$. The velocities in (ξ, η) co-ordinates are

$$\begin{aligned} U &= \xi_x u + \xi_y v, \\ V &= \eta_x u + \eta_y v, \end{aligned} \tag{6}$$

which represent the contravariant velocity components.

Flux splitting

The technique of flux vector splitting used in the present work was developed by Anderson *et al.*[12] and the flux is continuously differentiable even across eigenvalue sign changes, thus leading to smoother solutions at sonic and stagnation points. The two-dimensional Van Leer splitting flux can be formulated in general spatial co-ordinates ξ and η, but only the splitting for the flux $\hat{F}$ in the ξ-direction is given below since the others can be obtained similarly. The split flux $\hat{F}^{\pm}$ is given in terms of the local contravariant Mach number M_ξ, where $M_\xi = \bar{u}/a$ and $\bar{u} = U/|\text{grad}(\xi)|$.

For supersonic flow

$$\begin{aligned} \hat{F}^+ &= \hat{F} \quad \text{and} \quad \hat{F}^- = 0 \quad \text{if } M_\xi \geqslant 1 \\ \hat{F}^- &= \hat{F} \quad \text{and} \quad \hat{F}^+ = 0 \quad \text{if } M_\xi \leqslant -1, \end{aligned} \tag{7}$$

and for subsonic flow, $|M_\xi| \leqslant 1$,

$$\hat{F}^{\pm} = \frac{|\text{grad}(\xi)|}{J} \begin{bmatrix} f^{\pm}_{\text{mass}} \\ f^{\pm}_{\text{mass}}[\hat{k}_x(-\bar{u} \pm 2a)/\gamma + u] \\ f^{\pm}_{\text{mass}}[\hat{k}_y(-\bar{u} \pm 2a)/\gamma + v] \\ f^{\pm}_{\text{energy}} \end{bmatrix}, \tag{8}$$

where

$$f^{\pm}_{\text{mass}} = \pm \rho a (M_\xi \pm 1)^2/4, \tag{9}$$

$$f^{\pm}_{\text{energy}} = f^{\pm}_{\text{mass}} \{[-(\gamma-1)\bar{u}^2 \pm 2(\gamma-1)\bar{u}a + 2a^2]/(\gamma^2-1) + (u^2+v^2)/2\}. \tag{10}$$

$\hat{k}_x$ and $\hat{k}_y$ are the direction cosines of the interface in the ξ- and η-directions respectively and are defined as

$$\hat{k}_x = \xi_x/|\nabla\xi|, \qquad \hat{k}_y = \xi_y/|\nabla\xi|. \tag{11}$$

Spatial differencing

In the present flux-splitting method the spatial derivatives of fluxes $\hat{F}$ and $\hat{G}$ can be split into $\hat{F}^{\pm}$ and $\hat{G}^{\pm}$ in the general form

$$\delta_\xi \hat{F} = \delta_\xi^- \hat{F}^+ + \delta_\xi^+ \hat{F}^-, \qquad \delta_\eta \hat{G} = \delta_\eta^- \hat{G}^+ + \delta_\eta^+ \hat{G}^-, \tag{12}$$

where δ^+ and δ^- denote general forward and backward difference operators. In this approach the convective fluxes are evaluated at cell interfaces while the dependent variables are evaluated at the centroids. The split flux differences are implemented as a flux balance across a cell corresponding to MUSCL-type spatial differencing.[12] The spatial differencing of flux $\hat{F}$ in the ξ-direction can be defined as[13]

$$\delta_\xi \hat{F} = \frac{1}{\Delta\xi}[\hat{F}^+(Q^-_{i+1/2}, \vec{k}_{i+1/2}) - \hat{F}^+(Q^-_{i-1/2}, \vec{k}_{i-1/2}) + \hat{F}^-(Q^+_{i+1/2}, \vec{k}_{i+1/2}) - \hat{F}^-(Q^+_{i-1/2}, \vec{k}_{i-1/2})], \tag{13}$$

where $\hat{F}^{\pm}(Q^{\mp},\vec{k})$ denotes the split flux $\hat{F}^{\pm}$ and is evaluated by using the state variable $Q^{\mp}$ at the cell interface $(i\pm 1/2)$ and the normal direction cosine vector $\vec{k}$ $(\vec{k}\equiv\hat{k}_x\vec{i}+\hat{k}_y\vec{j})$. $Q^{\mp}_{i\pm 1/2}$ denotes the upwind-biased interpolation value at the interface of a computational cell. $Q^{+}_{i+1/2}$ is evaluated by Q_{i+2}, Q_{i+1} and Q_i (forward-biased) and $Q^{-}_{i+1/2}$ is evaluated by Q_{i-1}, Q_i and Q_{i+1} (backward-biased).

These interfacial values can be determined by the flux limiter, which is an important issue of the present work and will be discussed in the next sub-section.

Flux limiters and normalized variable diagram

For the MUSCL-type flux-splitting method the spatial differencing of the split flux can be first-, second- or even third-order-accurate if the interfacial values of $Q^{\pm}_{i\pm 1/2}$ are evaluated by a first-, second- or third-order interpolative method. If the interpolative function is not monotonic, an unreasonable value at the cell interface is obtained and the computational results exhibit oscillation (overshoot or undershoot) when discontinuity of the flow field is encountered. The use of switching functions (i.e. limiters) is an approach employed in Van Leer's flux-splitting method for this purpose. For simplicity, the subscripts of the dependent variables will be represented by the labels f, U, C and D from now on. These labels, defined in Reference 15, denote the nodal values downstream (D), central (C) and upstream (U) and the face value (f). The sense of 'upstream' or 'downstream' depends on the direction of the characteristic speed of the wave. For the backward-biased case Q_f is $Q^{-}_{i+1/2}$ and (Q_U, Q_C, Q_D) are (Q_{i-1}, Q_i, Q_{i+1}). For the forward-biased case Q_f is $Q^{+}_{i+1/2}$ and (Q_U, Q_C, Q_D) are (Q_{i+2}, Q_{i+1}, Q_i). Then the limiter can correlate the value of Q at the cell interface (f) and nodal points (U, C or D). For example, a general form of first/second-order upwind–weighted interpolation formula can be given as

$$Q_f = Q_C + \phi_f(Q_C - Q_U)/2. \tag{14}$$

The first- and second-order approximations correspond to $\phi_f = 0$ and $\phi_f = 1$ respectively, i.e. flux limiting is implemented through a spatial variation of ϕ_f.

The present work attempts to develop a flux limiter extended from the idea of Leonard, such as QUICK,[16] SHARP[15] or SMART.[14] These schemes are designed for convective modelling of discontinuities and applied to single-variable problems. A normalized variable diagram (NVD) is used to illustrate the relationship between the normalized convected control volume face variable and the normalized adjacent upstream node variable in these schemes. In the NVD plots, first- and second-order upwinding, second-order central differencing, QUICK, SHARP and SMART are all represented by different curves. Both accuracy and monotonicity are clearly shown by these functional relationships. The use of the NVD to express the flux limiter function is a new illustration of the flux limiter concept which gives an alternative physical essence. In order to equate the flux limiter of MUSCL-type flux-splitting methods and the NVD concept, all variables are unified in normalized form and the definition of the normalized variable is given as

$$\tilde{Q} = \frac{Q - Q_U}{Q_D - Q_U}. \tag{15}$$

Note that $\tilde{Q}_D = 1$ and $\tilde{Q}_U = 0$. Then the functional relation between the normalized convected face value $\tilde{Q}_f$ and the normalized adjacent upstream node value $\tilde{Q}_C$ can be obtained by the flux limiter function of equation (14) and the normalization of the dependent variables. The functional relations of the first-order upwind scheme,[11] the second-oeder upwind scheme,[17] the second-order CUI scheme,[18] QUICK,[16] SMART,[14] SHARP[15] and the third-order upwind-biased scheme of Van Leer[12] are given in Table I. These functions are plotted in Figure 1.

Table I. Functional relations between normalized interface value and adjacent node values for different schemes

Scheme	Functional relations ($\tilde{Q}_f$ versus $\tilde{Q}_C$)
First-order upwind[11]	$\tilde{Q}_f=\tilde{Q}_C$
Second-order upwind[17]	$\tilde{Q}_f=1{\cdot}5\tilde{Q}_C$
Second-order CUI[18]	$\tilde{Q}_f=\frac{5}{6}\tilde{Q}_C+\frac{1}{3}$
Third-order QUICK[16]	$\tilde{Q}_f=\frac{3}{4}\tilde{Q}_C+\frac{3}{8}$
Third-order SMART[14]	$\tilde{Q}_f=\tilde{Q}_C$ if $\tilde{Q}_C\notin[0, 1]$ $\tilde{Q}_f=3\tilde{Q}_C$ if $\tilde{Q}_C\in[0, \frac{1}{6}]$ $\tilde{Q}_f=1$ if $\tilde{Q}_C\in[\frac{5}{6}, 1]$ $\tilde{Q}_f=\frac{3}{4}\tilde{Q}_C+\frac{3}{8}$ if $\tilde{Q}_C\in[\frac{1}{6}, \frac{5}{6}]$
High-order SHARP[15]	$\tilde{Q}_f=\dfrac{\mathrm{SQRT}[\tilde{Q}_C(1-\tilde{Q}_C)^3]-\tilde{Q}_C^2}{1-2\tilde{Q}_C}$ if $\tilde{Q}_C\in[0, 0{\cdot}35]$ or $\tilde{Q}_C\in[0{\cdot}65, 1]$ $\tilde{Q}_f=\frac{3}{4}\tilde{Q}_C+\frac{3}{8}$ if $\tilde{Q}_C\in[0{\cdot}35, 0{\cdot}65]$ or $\tilde{Q}_C\in[-1, 1{\cdot}5]$ $\tilde{Q}_f=\frac{3}{8}\tilde{Q}_C$ if $\tilde{Q}_C\in[-1, 0]$ $\tilde{Q}_f=\tilde{Q}_C$ if $\tilde{Q}_C\in[1, 1{\cdot}5]$
Third-order Van Leer limiter[12]	$\tilde{Q}_f=\tilde{Q}_C+\dfrac{s}{4}\left(1+\dfrac{s}{3}(1-2\tilde{Q}_C)\right)$ where $s=\dfrac{2(1-\tilde{Q}_C)\tilde{Q}_C+\beta}{(1-\tilde{Q}_C)^2+\tilde{Q}_C+\beta}$, $\beta=10^{-6}$

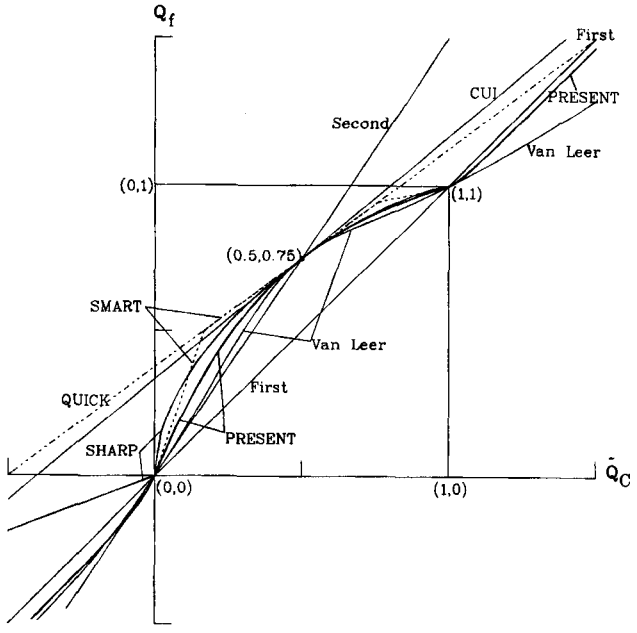

Figure 1. Normalized variable diagram

It is seen that the expressions of 'normalized limiters' in the SHARP and SMART algorithms consist of four or five piecewise functions and the computation of the intrinsic function SQRT is not economic. Moreover, these normalized limiters are not continuously differentiable, so that a problem of convergence is encountered when these limiter functions are used for a large time step.

The present work assumes that the normalized variable at the cell interface, $\tilde{Q}_f$, can be related to the normalized variable at the centroid, $\tilde{Q}_C$, as a fourth-order polynomial for $0 \leqslant \tilde{Q}_C \leqslant 1$ and two simple rational fraction functions with respect to $\tilde{Q}_C \leqslant 0$ and $\tilde{Q}_C \geqslant 1$. These functions are linked at points (0, 0) and (1, 1) with the same values of the first derivative. Thus the integrated expression of these functions is continuously differentiable. In order to assume the boundedness of the solution and the essential third order of accuracy, the polynomial follows the outline of a SMART algorithm and consists of the following features.

(i) A monotonic curve passes (0, 0), (0·5, 0·75) and (1, 1) with slopes S_{00} at $\tilde{Q}_C = 0$ and 0·75 at $\tilde{Q}_C = 0{\cdot}5$. The specified slope of 0·75 at $\tilde{Q}_C = 0{\cdot}5$ is desired so that the scheme is essentially third-order-accurate.[15]

(ii) The curve approaches the first-order upwind scheme if $\tilde{Q}_C$ is greater than unity or less than zero.

(iii) Convective stability and the convection boundedness criterion of Leonard must be satisfied.

The curves are described as follows:

$$\tilde{Q}_f = \begin{cases} \tilde{Q}_C[\tilde{Q}_C - S_{00}\beta_1]/(\tilde{Q}_C - \beta_1) & \text{for } \tilde{Q}_C \leqslant 0, \\ (10-4S_{00})\tilde{Q}_C^4 + (8S_{00}-19)\tilde{Q}_C^3 + (10-5S_{00})\tilde{Q}_C^2 + S_{00}\tilde{Q}_C & \text{for } 0 \leqslant \tilde{Q}_C \leqslant 1, \\ 1 + (\tilde{Q}_C - 1)[\tilde{Q}_C - 1 + (3-S_{00})\beta_1]/(\tilde{Q}_C - 1 + \beta_1) & \text{for } \tilde{Q}_C \geqslant 1. \end{cases} \tag{16}$$

where β_1 is a small value, chosen to be 0·05 in the present method. Accurate estimation of the interface value is of crucial importance where shock is encountered. Attention must be given to the selection of the limiter function of $\tilde{Q}_f$ near (0, 0) and (1, 1). An empirical formula for S_{00} is proposed:

$$S_{00} = \max[2{\cdot}7 - 1/(M_\infty^2 + 1), 2{\cdot}0]$$

This formula can reduce the value of S_{00} to 2·0 when the transonic flow field calculation is applied and quickly recover to 2·7 for increasing the resolution of strong shock for supersonic problems.

Characteristic-based variable

The use of the characteristic variable to evaluate the cell interface variable for the MUSCL procedure was first developed by Mulder and Van Leer.[19] They developed an implicit flux-vector-splitting procedure to solve the one-dimensional Euler equation which gives a different form of momentum equation. Three types of variable (conservative, approximately characteristic, true characteristic) to interpolate the cell interface value were applied for the averaging–limiting procedure for a single convection equation. Convergence was significantly improved with the true characteristic variable. The choice of characteristic variable for the flux limiter of this paper is extended from the local characteristic variable,[20] and the use of this characteristic variable in the MUSCL-type TVD scheme has been employed by Chakravarthy and Ota[21] to achieve high accuracy.

In Van Leer's original work,[12] conservative variables are the dependent variables as the flux limiter functions in all schemes. i.e. the interface values of the dependent variables are calculated by equation (14) and the flux limiter is a function of conservative variables of Q at the node points.

As a matter of fact, the adoption of primitive variables (i.e. ρ, u, v, p) instead of conservative variables as the dependent variables is an alternative method of using the flux limiter concept which might have been done in some computer programmes without discussion by the authors concerned. In this paper a new flux limiter is designed as a function of the characteristic variables of W at the node points. W is defined as follows:

$$W_U = \hat{R}_C^{-1} Q_U, \qquad W_C = \hat{R}_C^{-1} Q_C, \qquad W_D = \hat{R}_C^{-1} Q_D, \tag{17}$$

where $\hat{R}_C^{-1}$ are model matrices whose columns are eigenvectors of the Jacobian matrices $\hat{A}_C$ ($\equiv \partial \hat{F}/\partial \hat{Q}_C$). The model matrices are evaluated by the state variable Q_C and the direction cosine at the point C. In the present method the characteristic variables at the normalized cell interface, $\tilde{W}_f$, are first evaluated by the flux limiter functions (equation (16)) and related to the adjacent nodal value $\tilde{W}_C$ (i.e. all $\tilde{Q}$ in equation (16) are substituted by $\tilde{W}$). Furthermore,

$$W_f = \tilde{W}_f (W_D - W_U) + W_U. \tag{18}$$

Then the variables of Q_f can be obtained by multiplication of $\hat{R}_C$ (the inverse of $\hat{R}_C^{-1}$) and W_f, i.e.

$$Q_f = \hat{R}_C W_f. \tag{19}$$

Applications of the flux limiter based on characteristic variables W, conservative variables Q and primitive variables are compared in the present study. The next section shows that the characteristic-variable-based flux limiter leads to fast convergence and non-oscillatory solutions.

Implicit algorithm

The implicit algorithm is basically a backward Euler time integration scheme which uses approximate factorization in delta form as suggested by Beam and Warming,[22] i.e. equation (3) becomes

$$\left[I + \Delta t\left(\delta_\xi^- \frac{\partial \hat{F}^+}{\partial \hat{Q}} + \delta_\xi^+ \frac{\partial \hat{F}^-}{\partial \hat{Q}}\right)\right]^n \left[I + \Delta t\left(\delta_\eta^- \frac{\partial \hat{G}^+}{\partial \hat{Q}} + \delta_\eta^+ \frac{\partial \hat{G}^-}{\partial \hat{Q}}\right)\right]^n \Delta \hat{Q}_{i,j}$$
$$= -\Delta t(\delta_\xi^- \hat{F}^+ + \delta_\xi^+ \hat{F}^- + \delta_\eta^- \hat{G}^+ + \delta_\eta^+ \hat{G}^-)_{i,j}^n. \tag{20}$$

The spatial derivatives are approximated by MUSCL-type differencing with the newly designed limiter, and the flux Jacobian matrices $\partial \hat{F}^+/\partial \hat{Q}$, $\partial \hat{F}^-/\partial \hat{Q}$, $\partial \hat{G}^+/\partial Q$ and $\partial \hat{G}^-/\partial \hat{Q}$ are evaluated at the cell interface variable $Q_{i\pm 1/2}^{\mp}$. First-order upwind differencing is used on the left-hand side of equation (17) to yield a block-tridiagonal structure for the implicit equations; then the standard algorithm for solving this type of matrix equation can be used conveniently.

RESULTS AND DISUSSION

Three test problems were performed in order to verify the effectiveness of the flux limiters. The flux limiter proposed in the present study has several special features: (i) it is characteristic-based; (ii) it is essentially third-order-accurate, continuously differentiable; (iii) it is developed from the concept of NVD by Leonard.

The first test problem is a one-dimensional shock tube problem. For this problem the results computed by flux-splitting methods with the new and other flux limiters and by TVD methods are presented and compared. The different types of variables on which the flux limiters are based are tested and the results are compared against each other. The variables consist of conservative, primitive and characteristic variables.

The second test problem is a two-dimensional problem of an oblique shock step with Mach numbers 3 and 10 and a shock angle of 59°. It is probably the most severe test for any convective scheme. This is used for a comparison between SMART, SHARP and the third-order Van Leer flux-splitting method, all with characteristic-based flux limiters, and several TVD schemes. Oscillatory results with stability problems and the rate of convergence are also of interest. Nevertheless, the Mach number is much higher than for the other two test problems in this paper, which implies the existence of a strong shock.

The third test problem is a two-dimensional problem of transonic inviscid flow past an NACA0012 aerofoil with Mach number 0·8 at zero angle of attack. This computation is performed to prove that the present scheme is applicable to generalized co-ordinates and flow in the transonic range. The capability of capturing the shock wave by the present method can be thus demonstrated.

In order to shorten the length of the paper, the comparisons of the physical results by the flux limiters based on conservative and primitive variables are presented only for the one-dimensional shock tube problem. The physical results of other two test problems are illustrated with the flux limiter based on characteristic variables only.

Shock tube problem

The two-dimensional computational programme in this study can easily be simplified to a one-dimensional problem. The shock tube problem with the same initial conditions as in Reference 23 is shown in Figure 2. Initially, a diaphragm at $x=0{\cdot}5$ ($0 \leqslant x \leqslant 1$) separates two regions which have different densities ($\rho_L=1{\cdot}0$, $\rho_R=0{\cdot}125$) and static pressures ($p_L=1{\cdot}0$, $p_R=0{\cdot}1$) and the two regions are in a constant state and static ($u_L=u_R=0$). At time $t>0$ the diaphragm is broken and the case before any wave has reached the left or right boundary is considered. In the present computations, $\Delta x=0{\cdot}01$ and $\Delta t=0{\cdot}02$.

Figures 3 and 4 indicate the computed velocities and internal energies at $t=0{\cdot}14$ (i.e. after 70 time steps; denoted by symbols) by the SHARP, SMART, Van Leer and present algorithms employing the flux limiters based on conservative variables and their comparison with the exact solution (denoted by solid line). These figures show that the overshoots of the results obtained by SHARP are the largest of the four schemes, the next highest overshoot is shown by SMART, and then the present work and Van Leer's scheme. However, the results of SHARP and SMART exhibit higher shock resolution (the shock transition occupies three zones) than the results of the

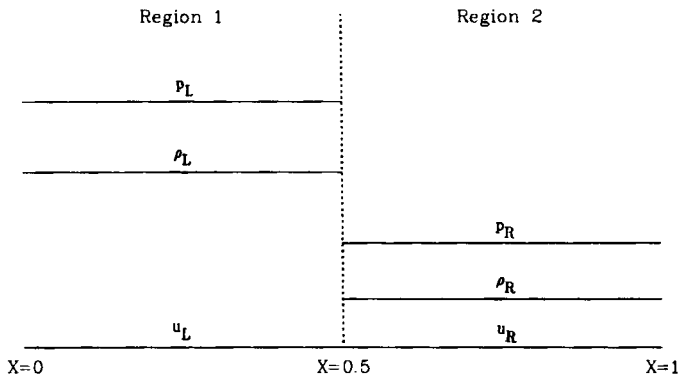

Figure 2. Initial conditions for 1D shock tube problem ($t=0$)

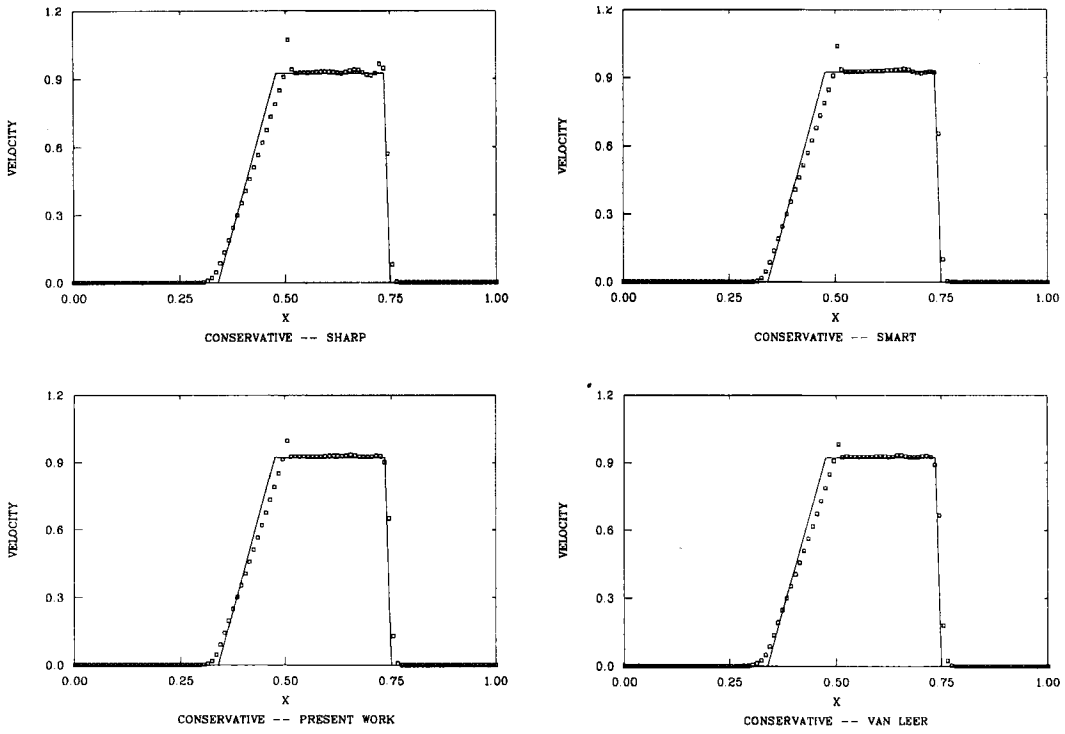

Figure 3. Computed velocities of 1D shock tube problem at $t=0{\cdot}14$ by different methods (limiter based on conservative variables)

present work and Van Leer's limiter (four and five zones respectively). This means that the present method gives slightly better accuracy (one mesh point near $x=0{\cdot}75$) than Van Leer's third-order scheme. Figures 5 and 6 show the velocities and internal energies obtained by the same algorithms with the flux limiter expressions based on primitive variables. It is obvious that the oscillatory behaviour is largely reduced and better accuracy is achieved. Note that the results of Figures 5 and 6 are obtained by the above-mentioned schemes with a primitive-based flux limiter; therefore the algorithms are not the same as those proposed in the original investigations. Figures 7 and 8 indicate that further reduction of the oscillatory behaviour and the best accuracy of the computed results are obtained by the flux limiter based on characteristic variables. The results of additional computations of the shock tube problem performed by Harten's second-order TVD scheme and Chakravarthy's third-order MUSCL-type TVD scheme are shown in Figure 9. The results of the two TVD schemes have no overshoots and undershoots and the shock resolution of the third-order scheme designed by Chakravarthy is better (the shock transition occupies five zones) than that of Harten's scheme (seven zones). Comparison of the results of Figures 8 and 9 indicates that the TVD schemes and the present scheme with a characteristic-based flux limiter give the same degree of successful prediction on internal energy but a very slight overshoot is still observed on velocity ($x\approx 0{\cdot}5$) by the present scheme. The following conclusions can be drawn from these figures. (i) the characteristic-based flux limiter eliminates a large portion of the oscillatory behaviour and the associated algorithms can give results with better accuracy than that of the conventionl conservative-based and primitive-based flux limiters. (ii) Although the present

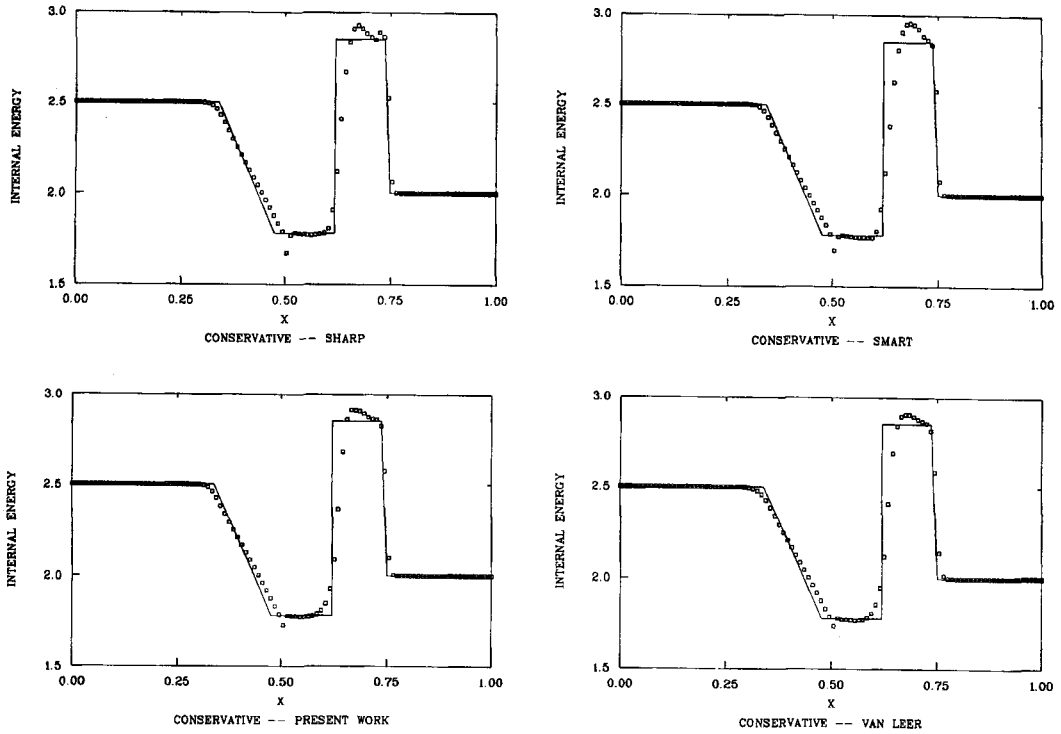

Figure 4. Computed internal energies of 1D shock tube problem at $t=0{\cdot}14$ by different methods (limiter based on conservative variables)

algorithm originates from the idea of the SHARP and SMART algorithms, the added property of continuous differentiability by a specially designed function improves not only the convergence rate but also the oscillation reduction. The accuracy of the results is close to or slightly better than that obtained by Van Leer's third-order scheme. (iii) The flux-splitting method with the proposed flux limiter based on characteristic variables can give the same good results as those of a second/third-order-accurate TVD scheme. On the basis of the above observations, the following two test problems are discussed mainly in the light of the flux-splitting method with a characteristic-based flux limiter.

Oblique shock step prpblem

The oblique shock step problem is a well-known test problem and the numerical results can be compared with exact solutions. The 24 x 24 grid system for the rectangular computational domain with a height : width ratio of 3 : 5 is uniformly distributed. The boundary conditions consist of: (a) a supersonic inflow at $i=1, j=1, \ldots, NJ$, which allows the values $Q_{1,j}$ to be fixed at free-stream conditions; (b) a prescribed fixed value of $Q_{i,1}$, $i=1, \ldots, NI$, which produces the desired shock strength and shock angle (59° in the present study); (c) a supersonic outflow at the rightmost surface ($i=NI=24, j=1, \ldots, NJ$) and the top surface ($j=NJ=24, i=1, \ldots, NI$), i.e. a zero-order extrapolation boundary condition can be used within these two boundaries.

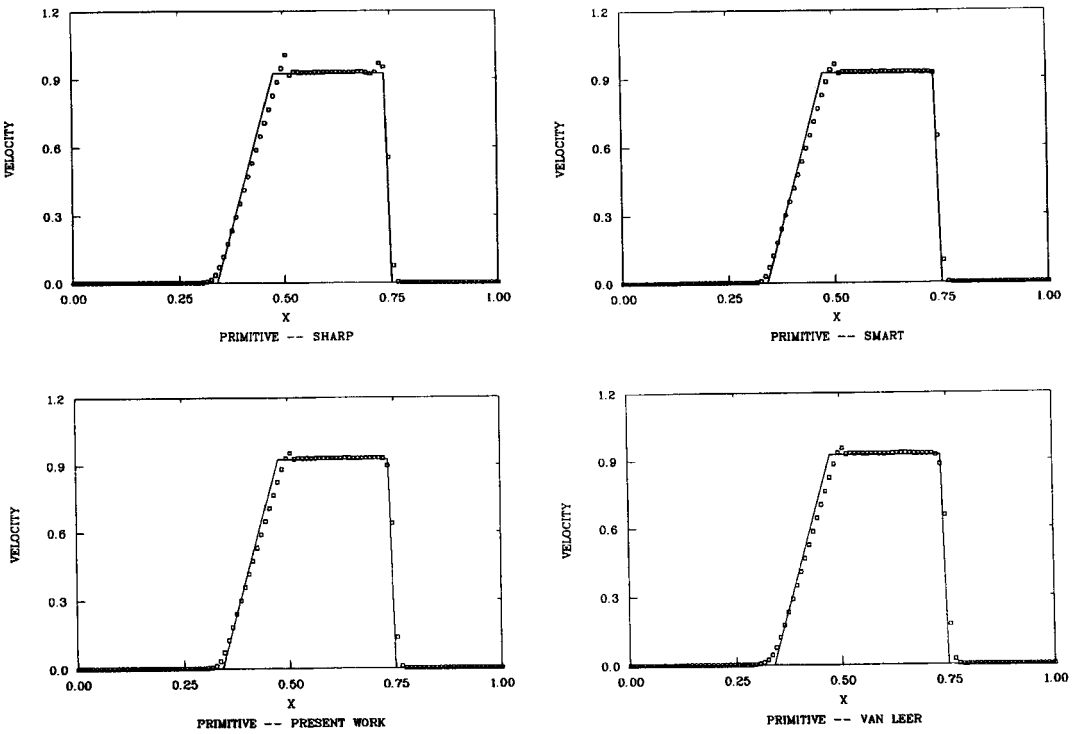

Figure 5. Computed velocities of 1D shock tube problem at $t=0{\cdot}14$ by different methods (limiter based on primitive variables)

Comparisons of the computational results by different characteristic-based 'flux limiters' of the SMART algorithm, the SHARP algorithm, the third-order Van Leer flux-splitting method, Harten's second-order TVD scheme, Chakravarthy's third-order MUSCL-type TVD scheme and the exact solution are made in terms of accuracy, oscillatory phenomena, stability and convergence rate.

Accuracy of solution and oscillatory phenomena. Figure 10(a) compares the results of the different schemes with the exact solution for a Mach number of 3. It must be noted that all schemes employ flux limiters based on characteristic variables and are therefore different from those of the original works. It is found that the SHARP and SMART algorithms yield more accurate results near $X/L=0{\cdot}5$ than the present scheme and Van Leer's scheme and even the two TVD schemes. The results of the TVD schemes show the poorest agreement with the exact solution (i.e. two points fall off the exact solution). All solutions have no overshoot or undershoot phenomena. When the Mach number is increased from 3 to 10 (Figure 10(b)), it is observed that the pressure results from the two TVD schemes and Van Leer's scheme are less accurate in front of the shock and improve somewhat behind the shock in comparison with the results of the other schemes. Although the SHARP algorithm gives the most accurate results of all the schemes, the time step must be reduced from CFL = 5·0 to 1·5 to get convergence for Mach number 10. This implies that convergence is difficult to obtain with the SHARP algorithm.

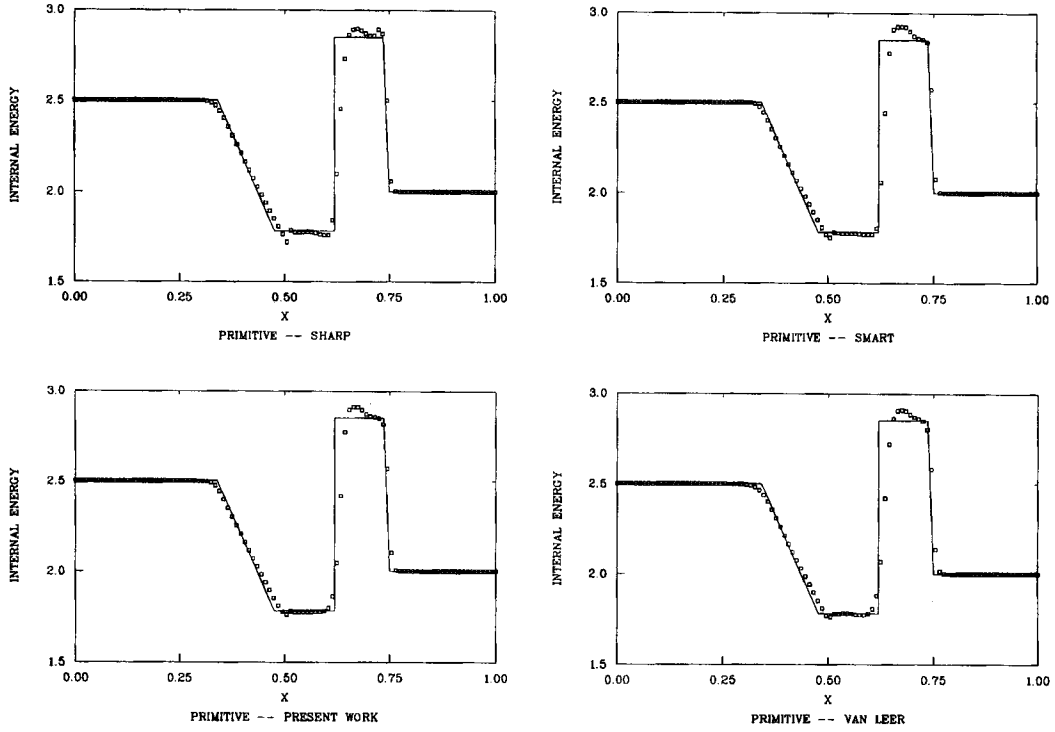

Figure 6. Computed internal energies of 1D shock tube problem at $t=0{\cdot}14$ by different methods (limiter based on primitive variables)

The accuracy of the computational results can be measured by the relative error ε in addition to the observed deviation from the exact solution in Figures 11(a) and 11(b). The relative error can be defined as

$$\varepsilon = \frac{\sum_{i=1}^{n} |P_i^{\text{calc}} - P_i^{\text{exact}}|}{\sum_{i=1}^{n} P_i^{\text{exact}}},$$

where P_i^{calc} is the calculated pressure at node i and P_i^{exact} is the exact solution for pressure at node i.

Figure 11(a) shows the histories of relative error for Mach number 3. It is found that the lowest errors are obtained with the SHARP and SMART schemes with small oscillation. Careful inspection of the values at each computational node shows that the error only exists at points adjacent to the shock location for the present method, the TVD schemes and the Van Leer flux-splitting method (third-order) (Figure 10(a) and 10(b)), i.e. the global relative errors are essentially induced by local errors of these points. Comparing the histories of relative error for Mach number 10 (Figure 11(b)) with those for Mach number 3, the accuracies of the computational results by the TVD schemes and Van Leer's method are close and the accuracy of the computed results by the present scheme is close to that by the SMART algorithm with the same CFL number. These figures indicate that the SHARP and SMART algorithms yield the best accuracy. The present proposed scheme gives results of a comparable degree of accuracy to the SHARP and

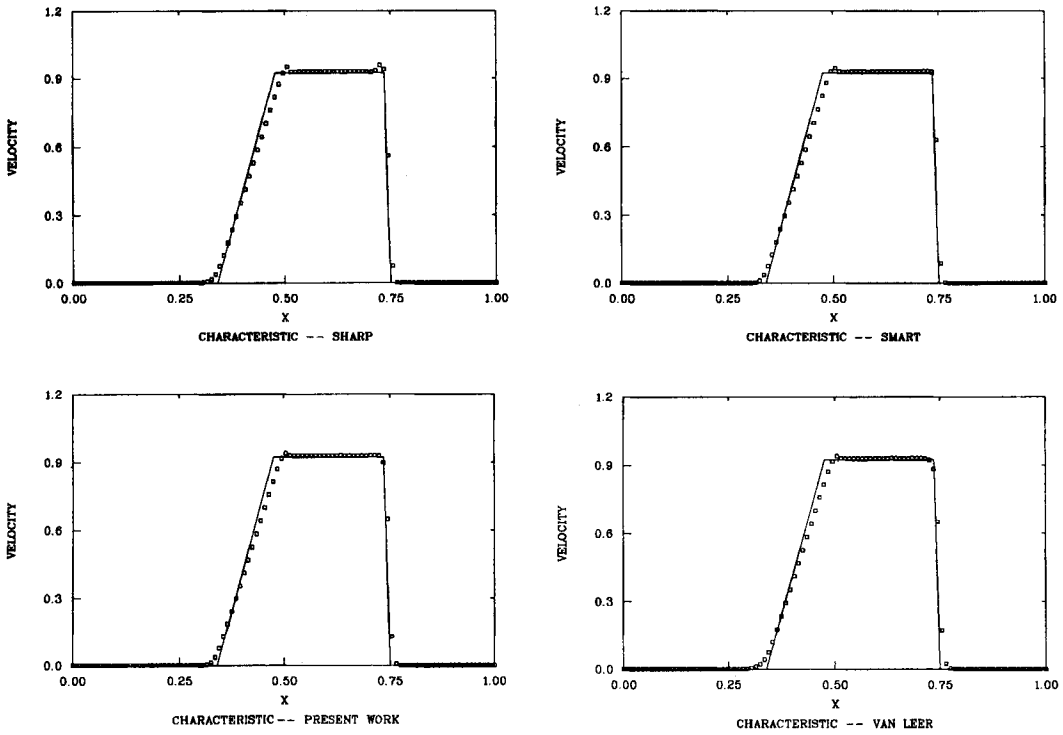

Figure 7. Computed velocities of 1D shock tube problem at $t = 0{\cdot}14$ by different methods (limiter based on characteristic variables)

SMART algorithms and with better agreement with the exact solution than the two TVD schemes and the Van Leer flux-splitting method.

Convergence histories. The residual history is an important consideration when selecting a numerical method. Figure 12(a) shows the residual histories for Mach number 3 and CFL = 5·0. It indicates that the convergence rates for the present method, the two TVD schemes and Van Leer's scheme are very close, but the residual value cannot be reduced to a level of less than 10^{-2} if the SHARP algorithm or 10^{-5} if the SMART algorithm is applied with a characteristic-based flux limiter. It is believed that the difficulty in convergence is associated with a discontinuous derivative of the limiter in certain regions and a steeper slope of $\tilde{Q}_f$ versus $\tilde{Q}_c$ near $\tilde{Q}_c \simeq 0$. Figure 12(b) plots the residual histories for Mach number 10. It shows that the high frequency of large scattering residual from the SHARP algorithm and the small scattering residual of the SMART algorithm still exist (even for CFL = 1·5 for the calculation by the SHARP algorithm). The rate of convergence of the present method is somewhat slower than that of Harten's TVD scheme but faster than the others.

Figures 12(c) and 12(d) compare the residual histories for the present scheme when the flux limiter is based on characteristic, primitive and conservative variables for Mach numbers 3 and 10 respectively. Figure 12(c) indicates that the reduction of residual value by the conservative-based and primitive-based flux limiters is slower than that by the characteristic-based flux limiter. Figure 12(d) shows similar results or Mach number 10 but more obvious conclusions are obtained.

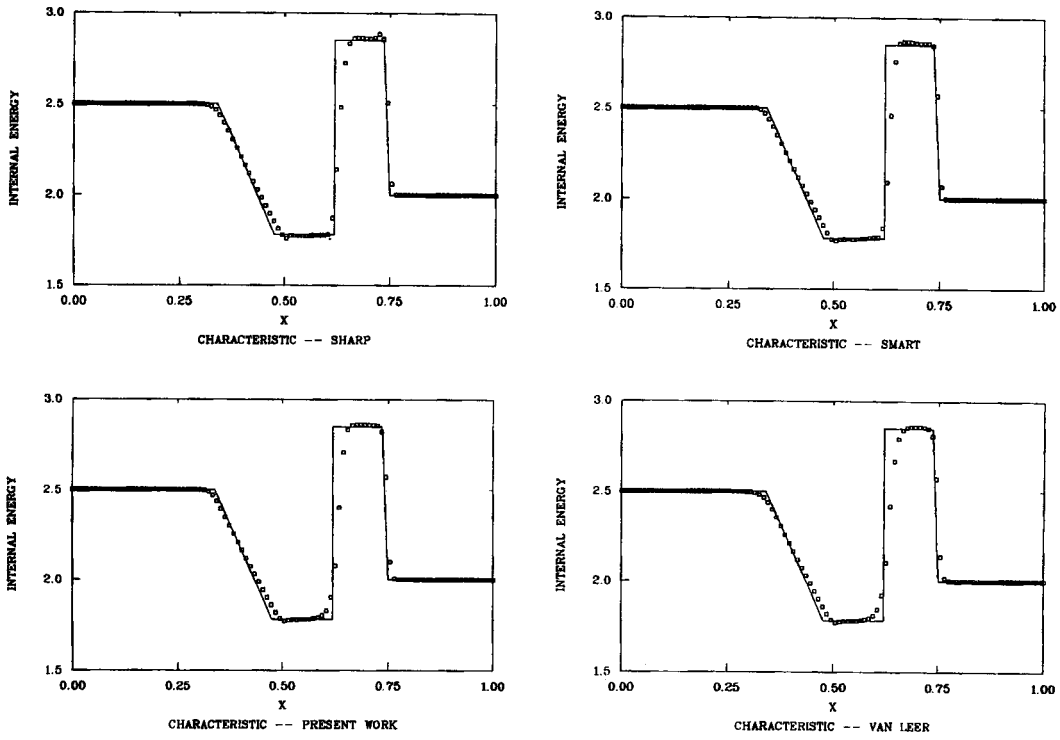

Figure 8. Computed internal energies of 1D shock tube problem at $t=0{\cdot}14$ by different methods (limiter based on characteristic variables)

Figures 12(c) and 12(d) imply that the choice of a characteristic-based flux limiter also provides desirable convergence characteristics.

In summary, for the oblique shock problem the proposed characteristic-based flux limiter of the present scheme provides results with slightly lower accuracy near the shock location but faster convergence rate than the flux limiters (Table I) of the SHARP and SMART algorithms. Also, the present method gives results of better accuracy than the Van Leer third-order scheme and the two TVD schemes of second/third-order accuracy, although they yield similar trends of convergence.

Computational results of transonic flow

A fully converged solution for the case of an NACA0012 aerofoil with $M_\infty = 0{\cdot}8$ at zero angle of attack is desired. A 96×32 half-C-type grid (Figure 13) is established by a hyperbolic grid solver for this problem. On the aerofoil surface the grid points are distributed with clustering at the nose, trailing edge and regions of shock so that the resolution of shock can be increased. The four boundary conditions are listed below:

(a) symmetric condition for $\xi = 0$
(b) outflow condition (subsonic) for $\xi = \xi_{\max}$
(c) inviscid wall condition (slip condition) for $\eta = 0$
(d) subsonic far-field condition for $\eta = \eta_{\max}$.

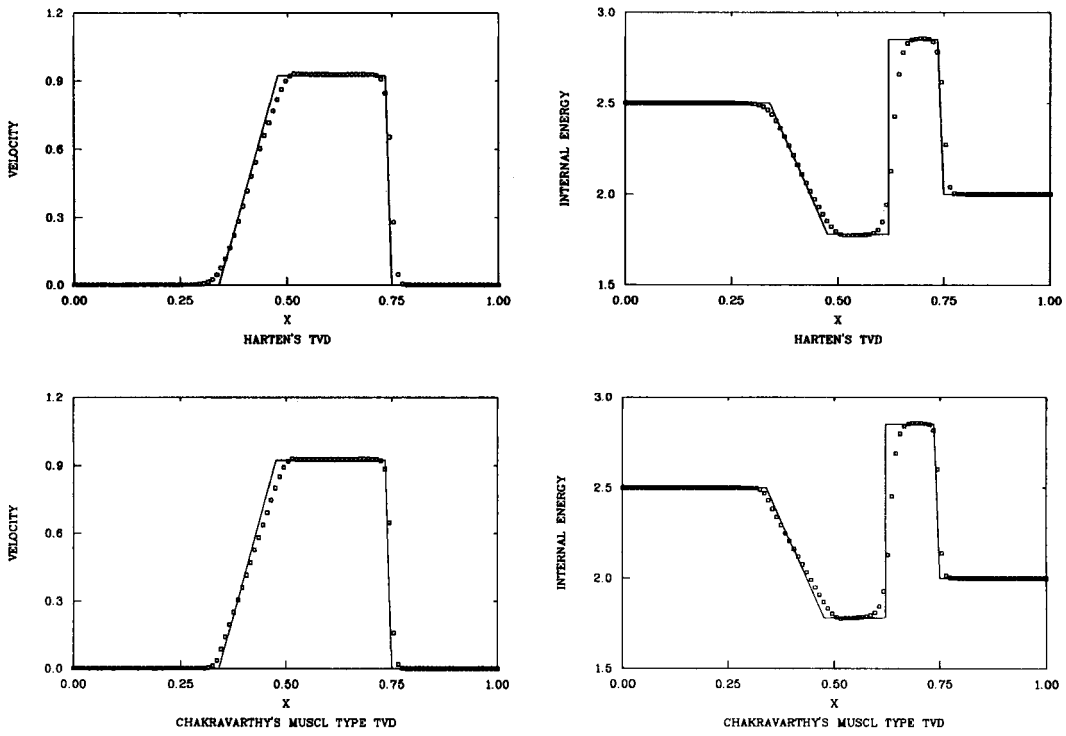

Figure 9. Computed velocities and internal energies of 1D shock tube problem at $t=0{\cdot}14$ by TVD schemes

A space-varying time step is used to accelerate convergence. The computed surface pressure coefficients (C_p) along the aerofoil are compared with the calculated results of Pulliam[24] in Figure 14. The computed values by the present method agree with Pulliam's data almost everywhere, except that Pulliam's results exhibit apparent 'undershoot' behind the shock while the present method achieves a non-oscillatory shock solution.

CONCLUSIONS

A characteristic-based flux limiter has been successfully developed to approximate the convective term at the cell interface in a third-order-accurate scheme. The oscillatory behaviour of the results is greatly reduced in comparison to a conservative-based or primitive-based flux limiter for all three test problems. The accuracy of the computed results by the present method is superior to that of a second/third-order TVD scheme and the Van Leer flux-splitting method with a smooth limiter; moreover, the accuracy of the results is comparable to that obtained by direct extension of the SMART or SHARP algorithm with characteristic-based flux limiters and to that from a third-order MUSCL-type TVD scheme. As applied to the oblique shock step problem with high Mach number, the present method provides the least amount of oscillation with a rapidly decreasing residual history and large CFL numbers. For transonic inviscid flow past an NACA0012 aerofoil, the present scheme can obtain a fully converged solution for Mach number 0·8 at zero angle of attack without an 'undershoot' pressure coefficient. Overall evaluations of the present method

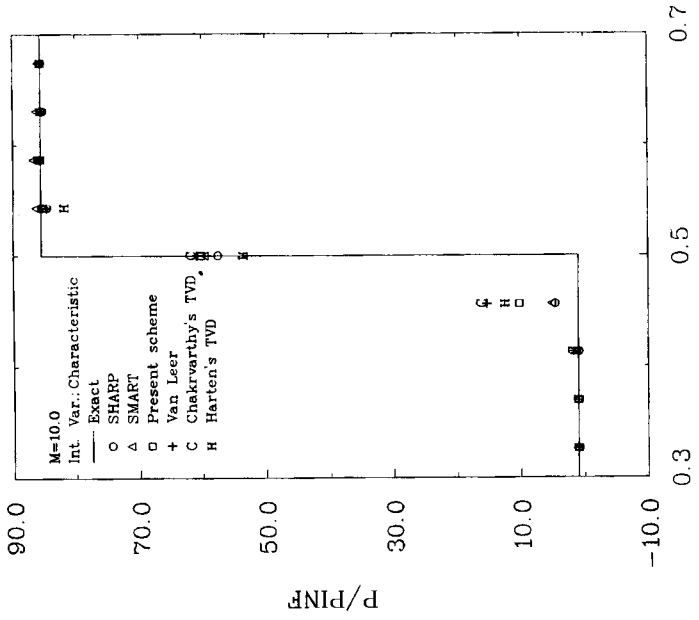

Figure 10(b). Computed static pressure at $y/H=0{\cdot}5$ by different schemes (oblique shock step problem, Mach number 10, shock angle 59°)

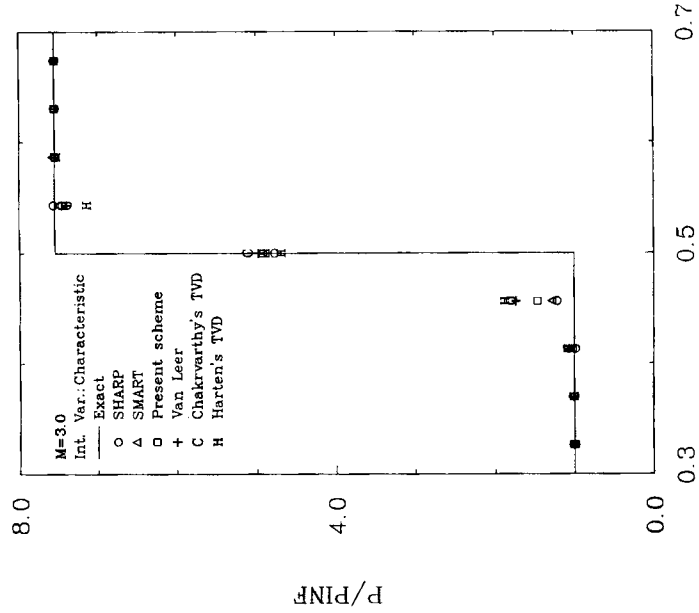

Figure 10(a). Computed static pressure at $y/H=0{\cdot}5$ by different schemes (oblique shock step problem, Mach number 3, shock angle 59°)

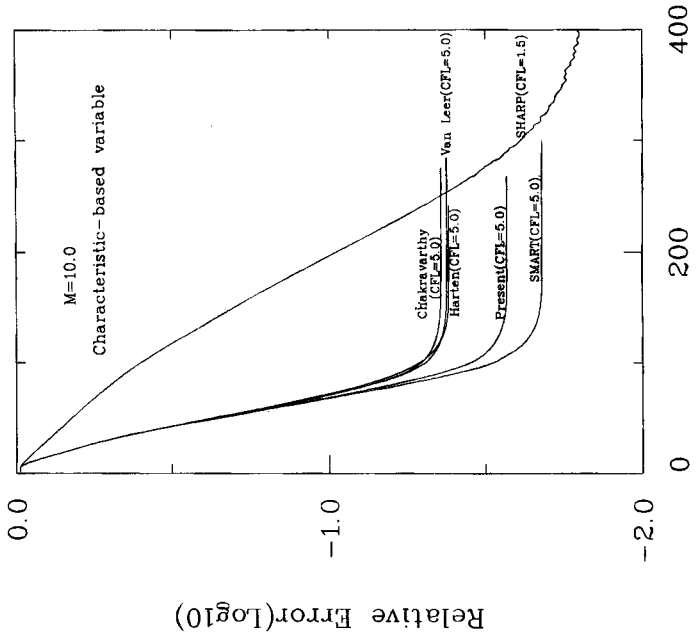

Figure 11(b). Relative error histories of oblique shock step problem by different schemes (Mach number 10)

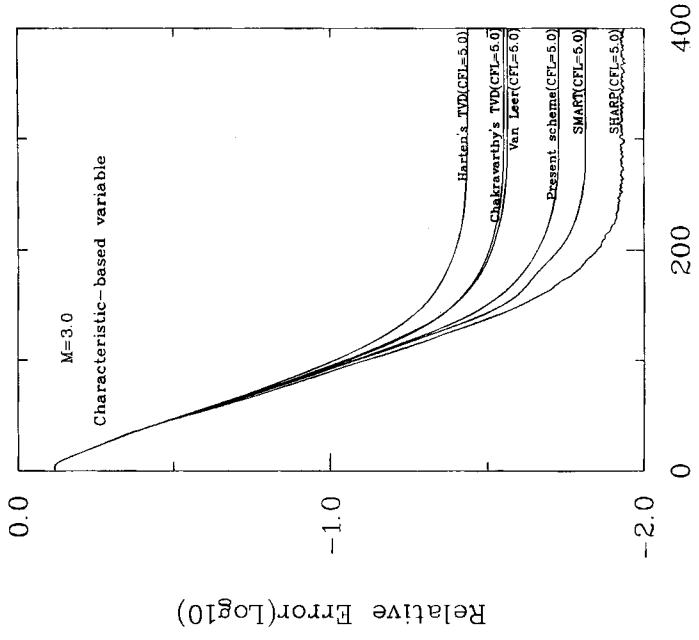

Figure 11(a). Relative error histories of oblique shock step problem by different schemes (Mach number 3)

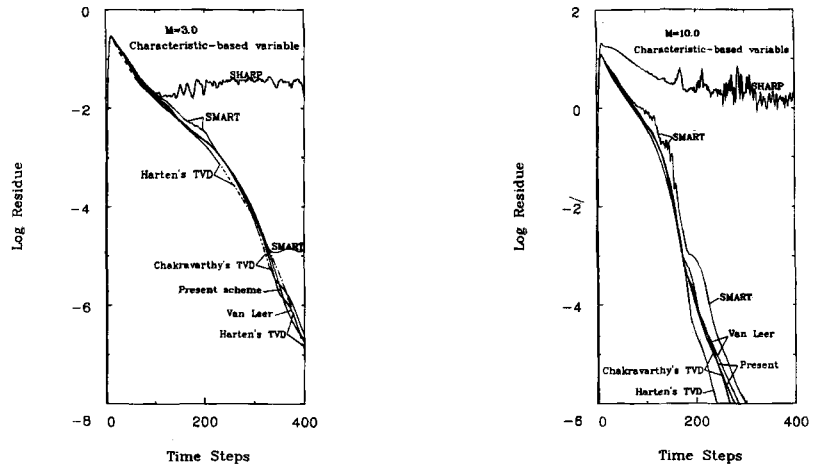

Figure 12. Residual histories of oblique shock step problem by different methods: (a) characteristic-based, Mach number 3; (b) characteristic-based, Mach number 10

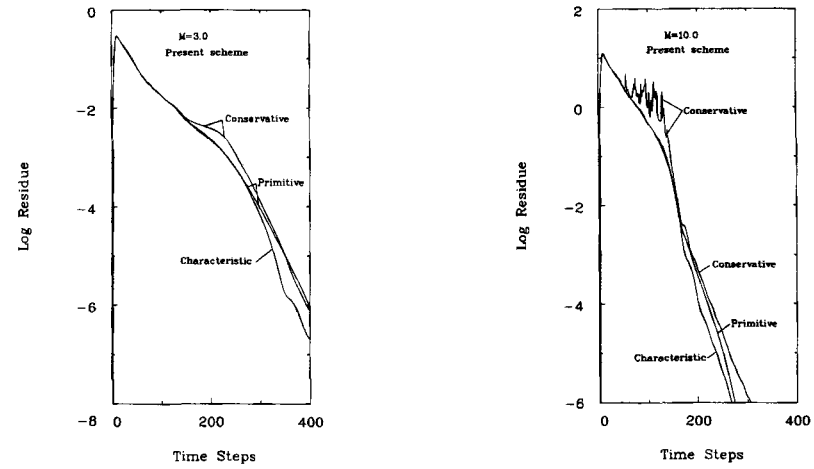

Figure 12. Residual histories of oblique shock step problem by present scheme (comparison between characteristic-based, primitive-based and conservative-based): (c) Mach number 3; (d) Mach number 10

prove that it provides non-oscillatory, accurate, fast-convergent results over a wide range of flow speed for the flux-splitting method.

APPENDIX: NOMENCLATURE

a	speed of sound
E_t	total energy per unit volume
F, G	fluxes of mass, momentum and energy
$\hat{F}, \hat{G}, \hat{Q}$	flux vector of transformed Euler equations
J	Jacobian of transformation

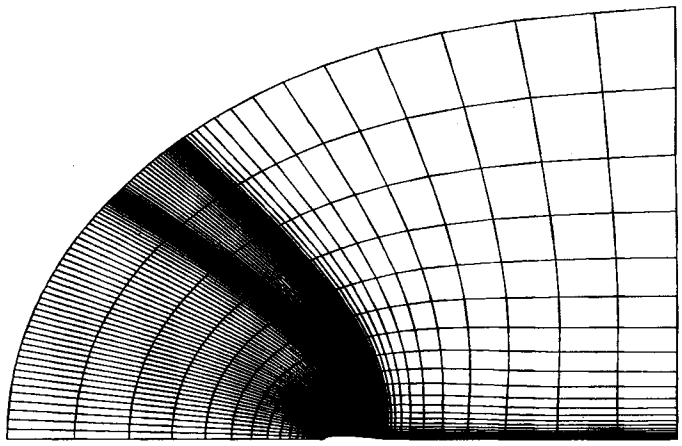

Figure 13. Computational grid of NACA0012 aerofoil for transonic inviscid flow problem

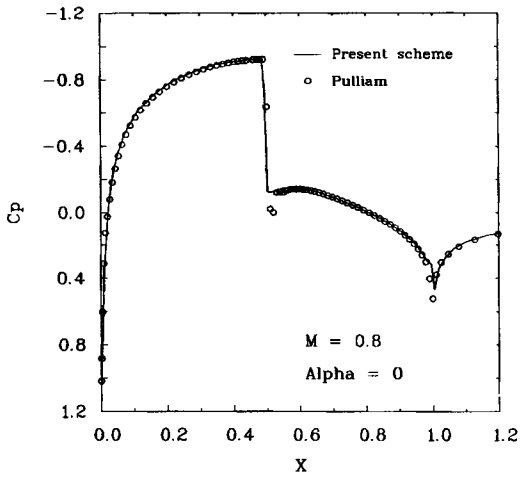

Figure 14. Computed surface pressure coefficients C_p of NACA0012 aerofoil by present scheme with Mach number 0·8 at zero angle of attack

$\hat{k}_x, \hat{k}_y$	direction cosines of interface in ξ- and η-directions
M	Mach number
p	pressure/$\rho_\infty a_\infty^2$
R	model matrix
S_{00}	slope value for present scheme
S_{11}	slope value for present scheme
t	time
u, v	Cartesian velocity components normalized by free-stream sound speed
U, V	contravariant velocity components normalized by free-stream sound speed
x, y	physical Cartesian co-ordinates
β	small value used for Van Leer's smooth limiter

β_1 small value used for present scheme
γ ratio of specific heats
δ_ξ first derivative in ξ-direction
δ_η first derivative in η-direction
δ^+ forward difference operator
δ^- backward difference operator
κ Van Leer limiter parameter; $\kappa = \frac{1}{3}$ for third-order limiter
ϕ scalar transport variable
$\bar{\phi}$ normalized transport variable
ξ, η transformed co-ordinates in streamwise and normal directions
ρ density normalized by free-stream density
Δt time increment
ε average error for test problem

Superscripts

$+, -$ positive and negative flux contributions; also forward and backward spatial differencing or extrapolation
n time level
$\tilde{(\ )}$ normalized variable

Subscripts

∞ free-stream condition
ξ streamwise direction
η normal direction
U upstream
D downstream
C centre
f cell interface

REFERENCES

1. H. C. Yee and A. Harten, 'Implicit TVD schemes for hyperbolic conservation laws in curvilinear coordinates', *AIAA J.*, **25**, 266–274 (1987).
2. A. Harten, 'High resolution schemes for hyperbolic conservation laws', *J. Comput. Phys.*, **49**, 357–393 (1983).
3. S. Osher and S. Chakravarthy, 'High resolution schemes and the entropy condition', *SIAM J. Numer. Anal.*, **21**, 955–984 (1984).
4. P. K. Sweby, 'High resolution schemes using flux limiters for hyperbolic conservation laws', *SIAM J. Numer. Anal.*, **21**, 995–1011 (1984).
5. P. L. Roe, 'Some contributions to the modeling of discontinuous flows', *Lect. Appl. Math.*, **22**, pt. II, 163–193 (1985).
6. H. C. Yee, R. F. Warming and A. Harten, 'Implicit total variation diminishing (TVD) schemes for steady-state calculations', *J. Comput. Phys.*, **57**, 327–360 (1985).
7. M. S. Liou, 'A generalized procedure for constructing an upwind-based TVD scheme', *AIAA Paper 87-0355*, 1987.
8. S. H. Chang, 'A comparison of ENO and TVD schemes', *Paper AIAA-88-3707, AIAA 8th Computational Fluid Dynamics Conf.*, 1988.
9. A. Harten and S. Osher, 'Uniformly high order accurate essentially non-oscillatory schemes III', *J. Comput. Phys.*, **71**, 279–309 (1987).
10. S. R. Chakravarthy and A. Harten, 'Essentially non-oscillatory shock-capturing schemes of arbitrary-high accuracy', *Paper AIAA-86-0339, AIAA 24th Aerospace Sciences Meeting*, Reno, 1986.
11. J. L. Steger and R. F. Warming, 'Flux vector splitting of the inviscid gasdynamics equations with application to finite-difference methods', *J. Comput. Phys.*, **40**, 263–293 (1981).
12. W. K. Anderson, J. L. Thomas and B. Van Leer, 'Comparison of finite volume flux vector splittings for the Euler equations', *AIAA J.*, **24**, 1453–1460 (1986).

13. D. B. Spalding, 'A novel finite difference formulation for differential expressions involving both first and second derivatives', *Int. j. numer. methods eng.*, **4**, 551–559 (1972).
14. P. H. Gaskell and A. K. Lau, 'Curvature-compensated convective transport: SMART, a new boundedness-preserving transport algorithm', *Int. j. numer. methods fluids*, **8**, 617–641 (1988).
15. B. P. Leonard, 'Simple high-accuracy resolution program for convective modeling of discontinuities', *Int. j. numer. methods fluids*, **8**, 1291–1318 (1988).
16. B. P. Leonard, 'A stable and accurate convective modeling procedure based on quadratic upstream interpolation', *Comput. Methods Appl. Mech. Eng.*, **19**, 59–98 (1979).
17. R. M. Beam and R. F. Warming, 'Upwind second-order difference schemes and applications in aerodynamic flows', *AIAA J.*, **14**, 1241–1249 (1976).
18. B. P. Leonard, 'A survey of finite differences of opinion on numerical modeling of incompressible defective confusion equation', *ASME, Applied Mechanics Division, Winter Annual Meeting*, 1979.
19. W. A. Mulder and B. Van Leer, 'Experiments with implicit upwind methods for the Euler equations', *J. Comput. Phys.*, **59**, 232–246 (1985).
20. H. C. Yee, 'Upwind and symmetric shock-capturing schemes', *NASA-TM-89464*, 1987.
21. S. R. Chakravarthy and D. K. Ota, 'Numerical issues in computing inviscid supersonic flow over conical delta wings', *AIAA Paper 86-0440*, 1986.
22. R. M. Beam and R. F. Warming, 'An implicit finite-difference algorithm for hyperbolic systems in conservation-law-form', *J. Comput. Phys.*, **22**, 87–110 (1970).
23. G. A. Sod, 'A survey of several finite difference methods for systems of nonlinear hyperbolic conservation laws', *J. Comput. Phys.*, **27**, 1–31 (1978).
24. T. H. Pulliam, 'An enhanced version of implicit code for the Euler equations', *AIAA Paper 83-0344, AIAA 21st Aerospace Science Meeting*, Reno, 1983.